

EFFECTS OF SIMULATED MICROMETEORITE BOMBARDMENT OF ROCK-FORMING SILICATES IN RAMAN SPECTRA. I. Weber¹, U. Böttger², M.P. Reitze¹, S.G. Pavlov², ¹Institut für Planetologie, Universität Münster, Wilhelm-Klemm-Str. 10, 48149 Münster, Germany. ²Institut für Optische Sensorsysteme, DLR; 12489 Berlin, Germany. (sonderm@uni-muenster.de)

Introduction: Our understanding of the composition of planetary surfaces and the processes that change them, such as space weathering (SW) caused by high-speed impacts, has been greatly enhanced by space missions. For in-situ missions with short-living landers, powerful analytical techniques came in front, such as Raman spectroscopy [e.g. 1]. A newly developed instrument is the Raman spectrometer for MMX - Martian Moons eXploration (RAX) [2], which is being developed for the in-situ exploration of the Martian moon Phobos.

In this laboratorial study, we investigate the influence of micrometeorite bombardment on bodies without atmosphere (such as Phobos) as one activator of SW on different silicates and their mixtures on Raman spectra. This SW effect is simulated with an excimer laser that irradiates the samples under low pressure. In a first SW study [3], we investigated the silicates olivine and enstatite and their mixtures, with the main result that laser irradiation reduced the fluorescence-dominated background signal (mainly olivine-related).

Here we present Raman spectroscopic data for mineral mixtures including feldspar (Table 1).

Methodology:

Samples: As possible components on celestial bodies without atmosphere, we formed the mixtures of the following rock-forming minerals:

Table 1: Compilation of the mixtures, wt%

Used mineral: Mixture ID	ID249 olivine	ID53 enstatite	ID22 diopside	ID28 plagioclase	ID13 quartz
359	10	12	19	59	-
360	11	24	4	61	-
361	100	-	-	-	-
362	49	1	36	11	3
363	63	-	37	-	-

Since we transfer all data to the Infrared and Raman for Interplanetary Spectroscopy (IRIS) database, each sample gets its own ID. After laser irradiation all samples got new IDs: ID359→364, ID360→365, ID361→366, ID362→367, ID363→368. For a good mixing result we used mineral powder with grain sizes of 63 µm to 125 µm. Smaller grain sizes would lead to agglutination and larger grain sizes are outside the range of regolith. However, in order to keep the essential part of the SW products (which would otherwise fly against the walls of the vacuum chamber) in the irradiated samples, the powders were

pressed into pellets (Fig. 1, left) in a hydraulic press with about 20 kN for approx. 25 minutes. This static pressure is sufficient to obtain stable pellets, but not to cause phase transitions. However, the individual grains are further crushed by pressing.

Characterization: For chemical and structural characterization, the minerals were carbon-coated before mixing and examined with an electron probe microanalyzer (EPMA; JEOL JXA 8530 F Hyperprobe) at the Institute for Mineralogy in Münster (analyses are available here: <http://bc-mertis-pi.uni-muenster.de/>). Images of the pellets before and after irradiation were done with a KEYENCE Digital Microscope VHX-500F (Fig. 1) and a JEOL JSM 6510-LV scanning electron microscope (SEM) (Fig. 2), both at the Institut für Planetologie (IfP).

Laser irradiation experiments: Micrometeorite bombardment was simulated in a special vacuum chamber [4]. The samples were irradiated with a 15-ns pulsed UV laser by series of 3 shots per point and at “starting” pressure in the chamber of 10^{-4} Pa. The energy density was determined between 1.64 J/cm^2 and 1.89 J/cm^2 over the whole area with a rectangular $300 \times 800 \mu\text{m}^2$ laser beam and an inner laser spot of $150 \times 140 \mu\text{m}^2$ in focus (Fig. 1).

Raman spectroscopy: All Raman measurements were performed with a confocal Raman microscope WITec alpha300R system at DLR (Berlin). Spectra were taken with a laser excitation wavelength of 532 nm at 3 mW, which is equal to $1.7 \text{ mW}/\mu\text{m}^2$ laser irradiation on the sample. This reflects the conditions of for example RAX on MMX. The spectral resolution is about 10 cm^{-1} . A Nikon 10 x objective was used with a light spot size on the pellets of about 1.5 µm. The samples were mounted on the XY motorized stage and step-scanned over the investigated area of $1000 \times 1000 \mu\text{m}^2$ with 50×50 matrix/points, which gives in total 2500 spectra per sample. Given by the roughness of the sample pellets, it is required to work statistically and with a medium focus.

Results: In the light microscope images (Fig. 1), the irradiated sample can be directly distinguished from the non-irradiated one by the darkened surface, especially in the olivine-dominated sample, indicating chemical decomposition. BSE images show the partly molten surface and the presence of nanophase Fe (Fig. 2c) in pyroxene. Plagioclase is mostly affected by laser irradiation showing extensive melting (Fig. 2d). Similar findings were reported for plagioclase [5] and enstatite [6]. Often the grains are fused by glass formation. In some places, small fused dots and glassy globules can be seen.

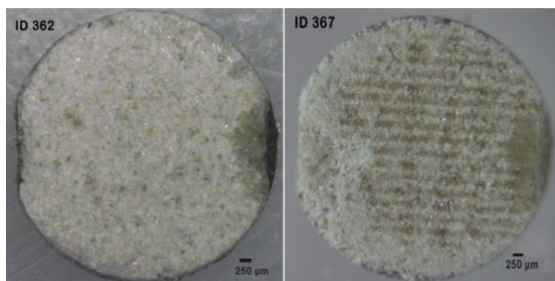


Fig. 1: Light microscope images of the ID 362 non-irradiated (left) and the related irradiated sample ID 367 (right), as an example. Laser shots appear as the darkened craters on the right.

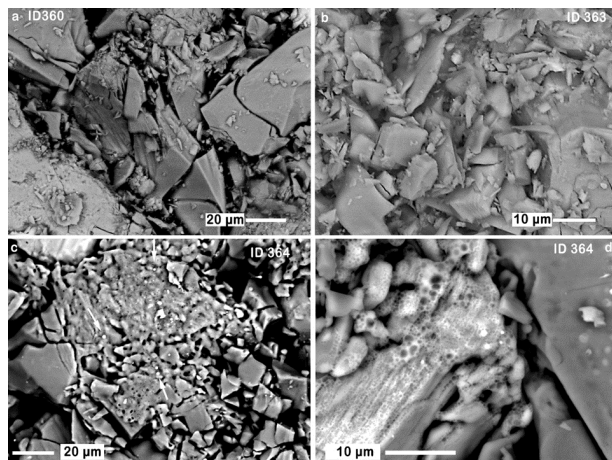


Fig. 2: Back-scattered electron (BSE) images of the non-irradiated samples ID 360 (a) and ID 363 (b), and the irradiated pellet ID 364 (c,d). c: Melted spherules and nanophase Fe, marked with an arrow, in pyroxene after irradiation are evident. d: Image of a molten plagioclase.

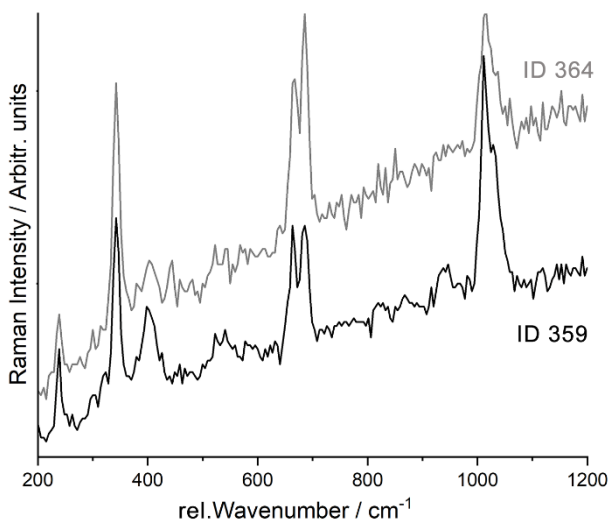


Fig. 3: Averaged Raman spectra of the non-irradiated (ID 359 black) and irradiated (ID 364 grey) samples in the range from 200 cm⁻¹ to 1200 cm⁻¹. Typical Raman shifts of the contained minerals can be seen.

In contrast to plagioclase, olivine and pyroxene mainly show the formation of nanophase iron due to their iron content [7,8]. Melting is present in the individual grains, but not as pronounced as in the plagioclase.

Raman spectra of the non-irradiated and irradiated samples in the Stoke range from 200 cm⁻¹ to 1200 cm⁻¹ show typical Raman lines of the mixed minerals (Fig. 3). The Raman lines did not change their position due to irradiation. However, if one compares the fluorescence histograms of the non-irradiated samples with those of the irradiated ones, a significant difference between plagioclase-rich and olivine-rich mixtures becomes apparent (Fig. 4).

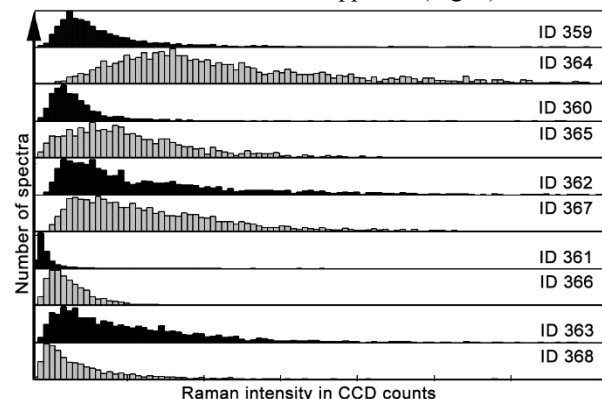


Fig. 4: Histograms of non-irradiated (black) and irradiated (grey) samples. The histograms describe the background intensity distribution of a sample area in CCD counts (X - axis) over the number of spectra (Y - axis) having a certain intensity. Each column in the histograms represents the number of spectra. The intensity is derived from each of 2500 spectra from 50 x 50 points on every sample.

Discussion: The aim of our study is to investigate whether and how Raman spectra are sensitive to micrometeorite bombardment as one source of SW. Our data of the minerals mixtures investigated in this study confirm the results of our previous study [3]; the fluorescence-dominated background signal is reduced in samples with a significant iron content. In plagioclase-rich samples the background fluorescence increases significantly. We assume that dense nanophase iron generally passivates luminescent atoms, such as rare-earth elements, in mineral mixes. The increased light in-depth penetration, e.g. in semi-transparent glassy (molten) phases may lead to increase of density of light-activated luminescent centers. These issues should be therefore considered in analysis of in-situ Raman spectra.

References: [1] Williford K.A. et al. (2018) *From Habit. to Life on Mars*, Ch. 11, 275–308. [2] Cho Y. et al. (2021) *Earth Planets Space* 73, 232. [3] Weber I. et al. (2021) *JRS* 53, 411–419.

[4] Weber I. et al. (2021) *EPSL* 569, 117072. [5] Moroz et al (2014) *Icarus* 235, 187–206. [6] Weber et al. (2020) *EPSL* 530, 115884. [7] Yamada et al. (1999) *Earth Planets Space* 51, 1255–1265. [8] Sasaki et al. (2003) *Adv. Space Res.* 31, 2537–2542. [9]

Additional Information: This work is partly supported by the DLR e.V. grant 50 QW 1701. The authors would like to thank U. Heitmann for sample preparation.